Dynamic collateral sensitivity profiles highlight challenges and opportunities for optimizing antibiotic sequences

Jeff Maltas[1], Anh Huynh[1], and Kevin B. Wood[1,2,*]

1 Department of Biophysics, University of Michigan, Ann Arbor, Michigan, United States of America
2 Department of Physics, University of Michigan, Ann Arbor, Michigan, United States of America

*kbwood@umich.edu

Abstract

As failure rates for traditional antimicrobial therapies escalate, recent focus has shifted to evolution-based therapies to slow resistance. Collateral sensitivity–the increased susceptibility to one drug associated with evolved resistance to a different drug–offers a potentially exploitable evolutionary constraint, but the manner in which collateral effects emerge over time is not well understood. Here, we use laboratory evolution in the opportunistic pathogen *E. faecalis* to phenotypically characterize collateral profiles through evolutionary time. Specifically, we measure collateral profiles for 400 strain-antibiotic combinations over the course of 4 evolutionary time points as strains are selected in increasing concentrations of antibiotic. We find that at a global level–when results from all drugs are combined–collateral resistance dominates during early phases of adaptation, when resistance to the selecting drug is lower, while collateral sensitivity becomes increasingly likely with further selection. At the level of individual populations, however, the trends are idiosyncratic; for example, the frequency of collateral sensitivity to ceftriaxone increases over time in isolates selected by linezolid but decreases is isolates selected by ciprofloxacin. Finally, we show experimentally how dynamic collateral sensitivity relationships can lead to time-dependent dosing windows that depend on finely timed switching between drugs.

Introduction

Evolution of resistance continues to reduce the available set of drugs for successful treatment of bacterial infections, cancers and viral infections [1–6]. As traditional maximum tolerable dose treatments fail at increasing rates, evolution-based treatments have emerged as a promising method to prolong the efficacy of current drugs or even reverse resistance. These treatments include drug cycling [7–10], harnessing spatial dynamics [11–14], cooperation [15–18], adaptive therapy [19–21], and judicious use of drug combinations [22–29]. More recently there has been a growing focus on exploiting collateral sensitivity to slow or reverse evolution in bacteria and cancer [30–39]. Collateral evolution occurs when a population evolves resistance to a selecting drug and as a direct result exhibits increased or decreased resistance to a different drug.

While collateral sensitivity is a promising evolutionary therapy, a number of factors make its application to the clinic challenging; for example, collateral effects exhibit a high degree of heterogeneity [40,41], distinct collateral profiles arise from different selection pressures [42], collateral effects are often not repeatable [43], and many non-antibiotic environments can confer collateral sensitivity [44–49]. Despite these challenges, theoretical and laboratory studies have shown that control theoretic

approaches may be used to counter, and even leverage, stochastic features of the evolutionary process to shape population outcomes [40,50]. Still, many fundamental questions about collateral sensitivity remain unanswered and are the focus of ongoing work. For example, the molecular mechanisms behind collateral sensitivity are known in relatively few cases [36,51], and it is unclear the extent to which collateral profiles are conserved across diverse species [52]. In addition, collateral drug pairs are difficult to identify in clinical settings, despite notable recent progress [53,54], and somewhat surprisingly, little is known about how collateral profiles change under continued selection, with much of the work performed only recently in other organisms such as cancer [37,55].

In this work, we sought out to understand how collateral effects change over time in bacteria exposed to increasing antibiotic selection and, in turn, how these potentially dynamic collateral sensitivity profiles may influence the design of drug scheduling. Using laboratory evolution in *Enterococcus faecalis*, a gram-positive opportunistic bacterial pathogen typically found in the gastrointestinal tracts of humans [56–61], we measure collateral sensitivity and resistance profiles over time for 20 populations exposed to increasing concentrations of five drugs, yielding 400 strain-antibiotic susceptibility measurement combinations. These collateral profiles reveal a complex story. When data from all drugs are combined, a clear trend emerges: collateral resistance appears more frequently in early stages of adaptation–when resistance to the selecting drug is lower–while further evolution increasingly favors collateral sensitivity. At the same time, collateral profiles are temporally dynamic and difficult to predict at the level of single drugs or single populations. Finally, we show experimentally that optimal drug scheduling may require exploitation of specific time windows where collateral sensitivity is most likely to occur. Taken together, our results underscore the importance of measuring temporal collateral profiles not only to better understand collateral evolution, but for any future work that hopes to harness collateral effects as a therapeutic option.

Results

Collateral effects are temporally dynamic

To investigate how collateral effects change over time in *E. faecalis*, we exposed four independent evolutionary replicates of strain V583 to escalating concentrations of a single drug over 8 days (approximately 60 generations) via serial-passage laboratory evolution (Fig 1, Materials and methods). In a previous study, we characterized collateral effects at the final endpoint of these evolutionary experiments [40]. In this work, we investigate the temporal progression of these collateral effects in a subset of five antibiotics chosen to represent a broad collection of mechanisms of action (Table 1). To do so, we isolated a single colony from each population at 2-day intervals and measured dose-response curves to each of the antibiotics (Fig 1A).

Table 1. Table of antibiotics used in this study and their targets.

Drug Name (Abbreviation)	Drug Class	Mechanism of Action
Ceftriaxone (CRO)	β-Lactam	Cell wall synthesis inhibitor
Ciprofloxacin (CIP)	Quinolone	DNA gyrase inhibitor
Daptomycin (DAP)	Lipopeptide	Cell membrane insertion
Doxycycline (DOX)	Tetracycline	30S protein synthesis inhibitor
Linezolid (LZD)	Oxazolidinone	50S protein synthesis inhibitor

We quantified resistance and sensitivity by estimating the half-maximum inhibitory dose (IC_{50}) for each strain-antibiotic combination (Materials and Methods). In total, we estimated the IC_{50} for 400 strain-antibiotic combinations (20 evolving populations,

measured against 5 antibiotics, at 4 evolutionary time points), each in (technical) replicates of three. For each measurement, we then calculated the collateral response $c \equiv \log_2 (\mathrm{IC}_{50,\mathrm{Mut}}/\mathrm{IC}_{50,\mathrm{WT}})$, the $\log_2$-scaled fold change in IC_{50} of the evolved strain relative to the ancestral V583 (Fig 1B). Resistance (direct or collateral) corresponds to $c > 0$ while sensitivity corresponds to $c < 0$ ($c = 0$ is indicated by the black dashed line). As in previous work [40,44], we defined collateral resistance or sensitivity to occur when the measured IC_{50} is at least 3 times the standard error of the mean of the wild-type ($|c| > 3\sigma_{WT}$, where σ_{WT} refers to standard error of the mean in the wild type; see Methods). While other definitions are possible, particularly in cases where a large number of technical replicates are available, we will see (below) that the qualitative trends we observe do not depend sensitively on the threshold for defining sensitivity or resistance.

Our results indicate that resistance to both the drug used for selection and the "unseen" testing drugs varies considerably over time. As expected, resistance to the selecting drug (diagonal entries, Figure 1B) tend to increase approximately (though not exclusively) monotonically over time and, in many cases, plateau after several days of selection. However, the temporal trends in collateral effects–the off-diagonal entries–are variable. In some cases, the population exhibits only collateral resistance (e.g. ciprofloxacin (CIP)-selected populations tested against ceftriaxone (CRO)) at all time points. In other cases, the same population exhibits collateral resistance at one time point and collateral sensitivity at another (e.g. ceftrixaone (CRO)-selected strains tested against doxycycline (DOX); Linezolid (LZD)-selected strains tested against CRO). Additionally, the variance in outcome across the 4 populations, and over time, depends on the testing drug. For example, resistance to DOX in all isolates varies over a relatively small range (fold-change in IC_{50} varies from a minimum of 0.4 to a maximum of almost 8), while resistance to CRO in the same strains varies substantially more (fold-change in IC_{50} varies from a minimum of 0.007 to a maximum of over 100). We also observe varying levels of induced collateral sensitivity between tested drugs. For example, at no point do any of the 20 evolved strains become collaterally sensitive to LZD, and collateral sensitivity to DAP is rare at all evolutionary time points. This is particularly notable because LZD and DAP are frequently used as last line of defense antibiotics in the treatment of multidrug resistant gram-positive infections [62–65].

Collateral effects are initially dominated by resistance but shift toward sensitivity with further adaptation.

To quantify how the propensity for collateral resistance changes over time, we calculated the "instantaneous" collateral resistance (or sensitivity), which measures collateral effects at each time point *relative to the previous time-point*, rather than relative to the ancestral strain (Fig 2). For example, to investigate how the population changed between days 4 and 6 we calculate: $c_{\mathrm{inst}} \equiv \log_2 (\mathrm{IC}_{50,\mathrm{D6Mut}}/\mathrm{IC}_{50,\mathrm{D4Mut}})$, where the IC_{50}'s are calculated at days 6 and 4. This analysis reveals that the first two days of evolution are dominated by collateral resistance effects (91.25%), while the subsequent 6 days of evolution confer collateral resistance at considerably reduced frequencies (33.75%, 38.75%, and 32.50% respectively). Further, after the first two days of evolution, the last 6 days also share a similar frequency of collateral sensitivity (52.5%, 55.0%, and 57.5% respectively).

To further quantify these trends, we combined the data from all drugs and all time points and calculated the mean instantaneous collateral effects as a function of resistance to the selecting drug (Figure 2C, left panel; see also Figure S1 for cumulative collateral effects). At this global level, the mean collateral effects (both instantaneous and cumulative) trend downward–toward sensitivity and away from resistance–as

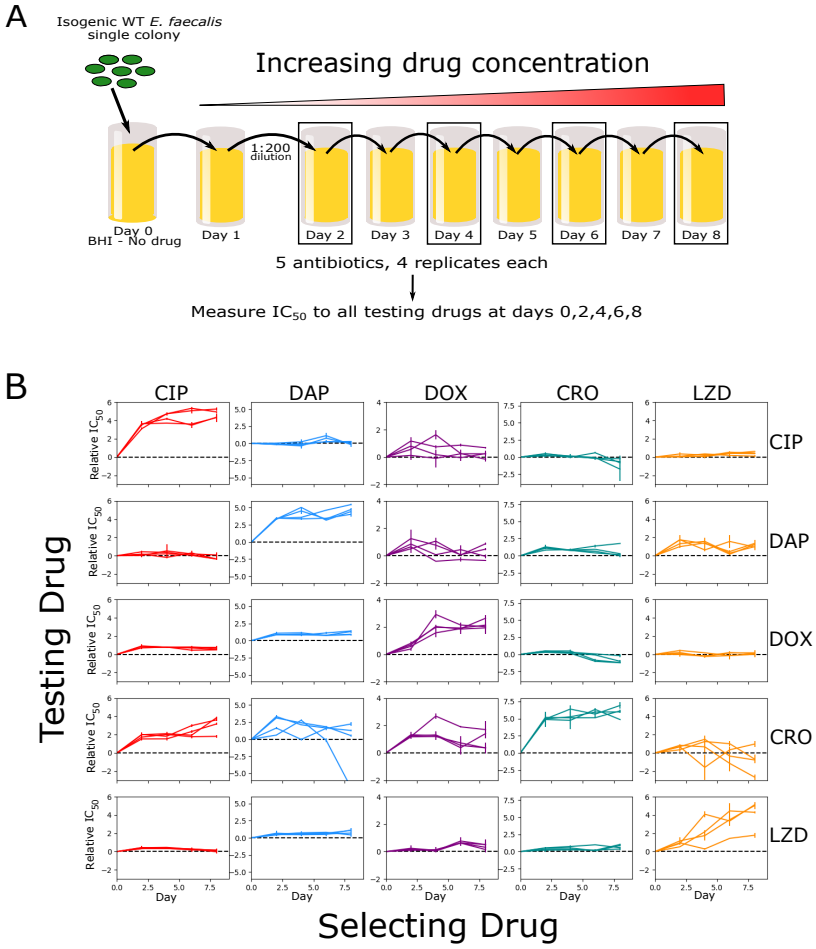

Fig 1. Laboratory evolution of *E. faecalis* reveals diverse, temporally dynamic collateral sensitivity profiles. (A) *E. faecalis* strain V583 was exposed to single antibiotics in escalating concentrations over the course of an 8-day serial-passage evolution experiment (roughly 60 total generations). Four independent populations were evolved in the presence of one of five selected antibiotics. The half-maximal inhibitory concentration (IC_{50}) was estimated for a single isolate from each population at days 2, 4, 6 and 8. **(B)** Resistance/sensitivity measurements taken every two days for each of the 20 mutants to each of the 5 antibiotics quantified by the $\log_2$-transformed relative increase in the IC_{50} of the testing drug relative to that of WT V583 cells (black dashed line at $y = 0$). Rows represent the drug used to select the mutant (selecting drugs: Ciprofloxacin (CIP) = red, Daptomyacin (DAP) = blue, Doxycycline (DOX) = purple, Ceftrixone (CRO) = teal, Linezolid (LZD) = orange), whereas columns represent the drug used in the testing assay. Error bars represent the standard error of the mean (SEM) for each individual experiment. Note that the y-scales are different for each column but the same within a column to allow for comparison of collateral effects (off-diagonal) with direct effects (diagonal).

resistance to the selecting drug increases. Notably, the *instantaneous* collateral resistance at early stages (when resistance to the selecting drug is small) is sufficiently large that the mean *cumulative* collateral effects remain positive even at later stages (Figure S1, left); that is, the trend toward collateral sensitivity is not strong enough to overcome the initial collateral resistance acquired at low levels of resistance to the selecting drug.

Similarly, the probability (frequency) of collateral sensitivity increases (Figure 2C, right panel; Figure S1; $p_{\text{value}} < 0.05$ from logistic regression, see Methods and SI Supplemental Tables) and the probability of collateral resistance decreases (Figure S2, $p_{\text{value}} < 0.05$) as resistance to the selecting drug is increased. These qualitative trends do not depend sensitively on the specific thresholds used to define CS/CR (Figure S3).

One simple explanation of this phenomenon may be an abundance of easily accessible, low-level resistance mutations, perhaps related to efflux pumps [66–68] or a general stress response [69,70], that broadly confer low-level multidrug resistance at early stages of adaptation. As the antibiotic concentration is increased the population is required to evolve more antibiotic-specific mutations that may be associated with collateral trade-offs.

Temporally dynamic collateral effects are difficult to predict at the level of individual drugs.

While global trends emerge when the data from all drugs is combined, it is not clear whether similar trends occur at the level of individual drugs. To investigate this question, we first calculated correlations between each of the 5 testing conditions (Fig S4A) to search for statistical similarities between different drugs. Depending on the metric used, we find that either 4 or 5 of the 10 pairwise combinations produce a statistically significant but relatively weak negative correlation. However, scatter plots indicate that these relationships are nonlinear with considerable scatter, even when statistically significant.

In addition, we found that collateral effects for specific drugs are difficult to predict from collateral profiles measured at earlier times in the same strain. For example, one DAP-adapted population exhibits a significant increase in resistance to CRO between days 2 and 4, however days 4 to 6 and 6 to 8 both come with a significant collateral sensitivity. Similarly, the LZD-selected strains confer resistance to DAP on days 2 and 8, but exhibit collateral sensitivity on days 4 and 6. To quantify this effect, we calculated how often an observation from the current time step correctly predicted change in resistance measurement two days later. That is, if a particular isolate exhibited collateral sensitivity to a drug on day 2, how frequently did it also exhibit collateral sensitivity on day 4? Somewhat surprisingly, collateral profiles on day 2 correctly predict only 41% of day 4 collateral profiles. Similarly, day 4 only successfully predicted 37% of day 6 collateral profiles and day 6 accurately predicted 41% of day 8 profiles. These data indicate that, in contrast to resistance levels to the selecting drug, which tend to be non-decreasing over time, instantaneous collateral effects are largely uncorrelated after short periods (2 days; 10-20 generations) of adaptation. This lack of predictability might also arise if populations are largely heterogeneous over time, meaning that sampling single colonies from each population could result in the appearance of dynamic or stochastic evolution.

Collateral effects are dynamic within individual populations.

To investigate heterogeneity within the evolving populations, we focused on three selection-testing drug pairs (LZD-CRO, CRO-DOX, and CRO-CIP), which correspond to lineages adapted to one of three drugs (LZD, CRO, and CIP) and tested against a

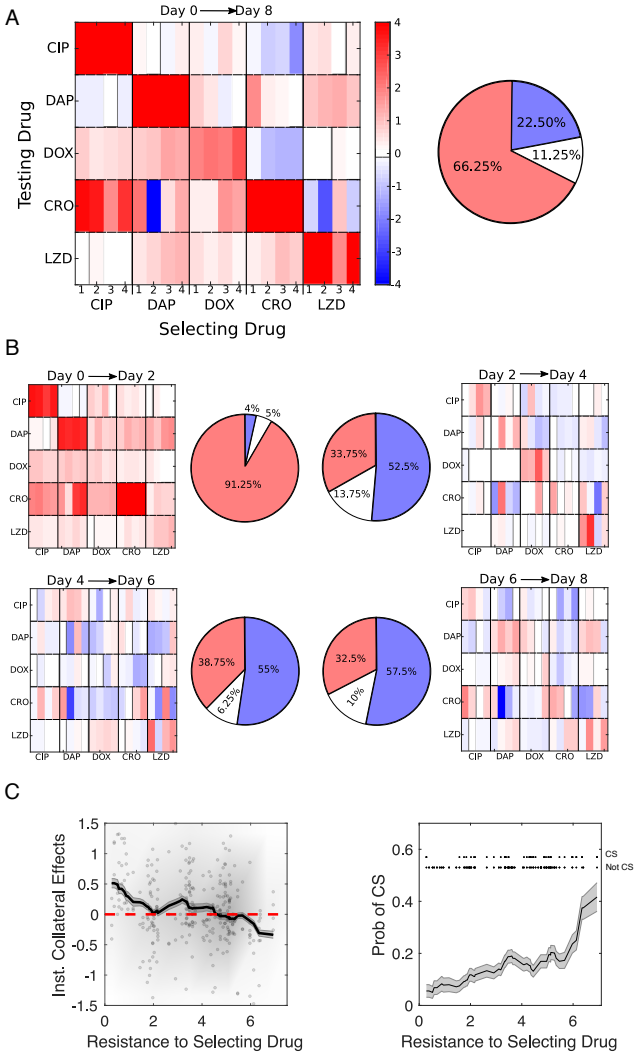

Fig 2. Early evolution is dominated by collateral resistance followed by a diverse set of collateral responses as evolution continues. (A) Left: Collateral profiles measured at the final time point (day 8), relative to the day 0 ancestor. Resistance (red) or sensitivity (blue) to each antibiotic is quantified via the $\log_2$-transformed fold change in IC_{50} relative to the ancestral strain (V583). A measurement is deemed to be collaterally resistant or sensitive if it falls above or below 3 times the standard error of the mean of the wild-type ($|c| > 3\sigma_{WT}$). For each selecting drug, there are 4 evolutionary replicates (thin rectangular columns). **Right:** Pie chart representing the fraction of collateral effects that confer resistance (red), sensitivity (blue) or no statistical change (white/gray). **(B)** Instantaneous collateral effects: collateral profiles measured for the same 20 mutants as A, but collateral sensitivity/resistance is defined relative to the previous time point (rather than the ancestor strain). Days 0-2, top left; days 2-4, top right; days 4-6, bottom left; days 6-8, bottom right. Over 90 percent of collateral effects conferred between days 0-2 resulted in collateral resistance. The subsequent 6 days of evolution (days 2-4, 4-6, and 6-8) only conferred collateral resistance 34%, 39% and 33% respectively. **(C)** Instantaneous collateral effects (i.e. collateral effects relative to previous timepoint) (left) and probability of collateral sensitivity (CS) (right) as a function of resistance to selecting drug. Left panel: dots are individual populations, shading indicates relative density of points, and curve is moving average (shading is $\pm$ standard error over each window). Right panel: curve is moving average (shading is $\pm$ standard error over each window). Upper inset shows individual data points (top row is CS, bottom row is not CS) used to calculate probability. Averages are performed over windows of size 2. See also Figures S1, S2, S3 and SI.

different drug (CRO, DOX, and CRO, respectively). In two examples (LZD-CRO and CRO-DOX), the original data suggested collateral resistance to the testing drug decreases over time, with resistance occurring at early stages and sensitivity at later stages. In the third example (CRO-CIP), the collateral effects are approximately constant (resistance) over time.

From each of the three populations, we isolated 48 colonies (12 colonies from each of 4 time points) and measured the response of each isolate to the testing drug using dose response curves (Figure 3). We found that the specific distributions of IC_{50} values vary in idiosyncratic ways–for example, the LZD-CRO population is characterized by a roughly unimodal distribution whose mean decreases over time, while the CRO-DOX population is characterized by coexistence of highly resistant and highly sensitive isolates at early times, while later time points contain primarily sensitive isolates. Indeed, the mean collateral resistance (i.e. fold change in IC_{50} relative to ancestor) is dynamic–specifically, it is not the same at every time point in the LZD-CRO (1-way Anova, $p_{\text{value}} = 0.0008$), CRO-DOX ($p_{\text{value}} = 0.001$), and CIP-CRO pairs ($p_{\text{value}} = 0.05$). See SI for pairwise comparisons at all time points.

In addition, we calculated the frequency of CR and CS across isolates. We found that the frequency of sensitive isolates increases over time in the LZD-CRO and CRO-DOX pairs (logistic regression, $p_{\text{value}} = 0.04$ and $p_{\text{value}} = 0.005$, respectively; see Methods) and the frequency of resistant isolates decreases in the LZD-CRO pair ($p_{\text{value}} = 0.007$; for CRO-DOX the trend is qualitatively similar but not significant, $p_{\text{value}} = 0.1$). In contrast to the first two populations, the third population (CRO-CIP) shows the opposite trend, with resistance increasing in frequency ($p_{\text{value}} = 0.05$) and sensitivity decreasing in frequency over time ($p_{\text{value}} = 0.02$).

These results indicate that the adapting populations exhibit heterogeneity in collateral resistance profiles but nevertheless show clear temporal trends, even within single populations. In some cases (LZD-CRO, CRO-DOX), the trends are reminiscent of the global trends observed across drugs–that is, early stages of adaptation favor collateral resistance and later stages collateral sensitivity–but this is by no means universal (e.g. CRO-CIP exhibits opposite trends).

Simple model highlights potential trade-offs of multi-drug sequences when collateral profiles are dynamic.

Our results raise the question of whether dynamic collateral sensitivity may jeopardize otherwise effective drug sequences, especially those involving multiple drug switching events. To investigate this question, we developed a simple model (SI) that corresponds to the accumulation of independently combined, but dynamic, collateral effects–intuitively, this could represent a single dominant lineage that sequentially acquires multiple mutations over time. We stress other evolutionary processes are certainly possible, and even likely under some conditions–for example, adaptation may be dominated by a single selection step that enriches for specific mutants from a heterogeneous population. Our goal is not to investigate these dynamics in detail, but simply to provide a null model that quantifies the potential combinatorial patterns associated with the dynamic collateral profiles we measured. In this model, the trends we observe experimentally–namely, the enrichment for resistance at early stages of adaptation–mean that switching between drugs is not always beneficial (Figure S6). Instead, switching gives rise to a trade-off: optimal sequences may minimize the resistance to the applied drug (similar to results observed experimentally in [40]), but adding additional drugs tends to raise the global resistance levels–that is, the cumulative resistance of the population to the set of all available drugs. This global resistance does not depend sensitively on the timing of the drugs, though it is precisely

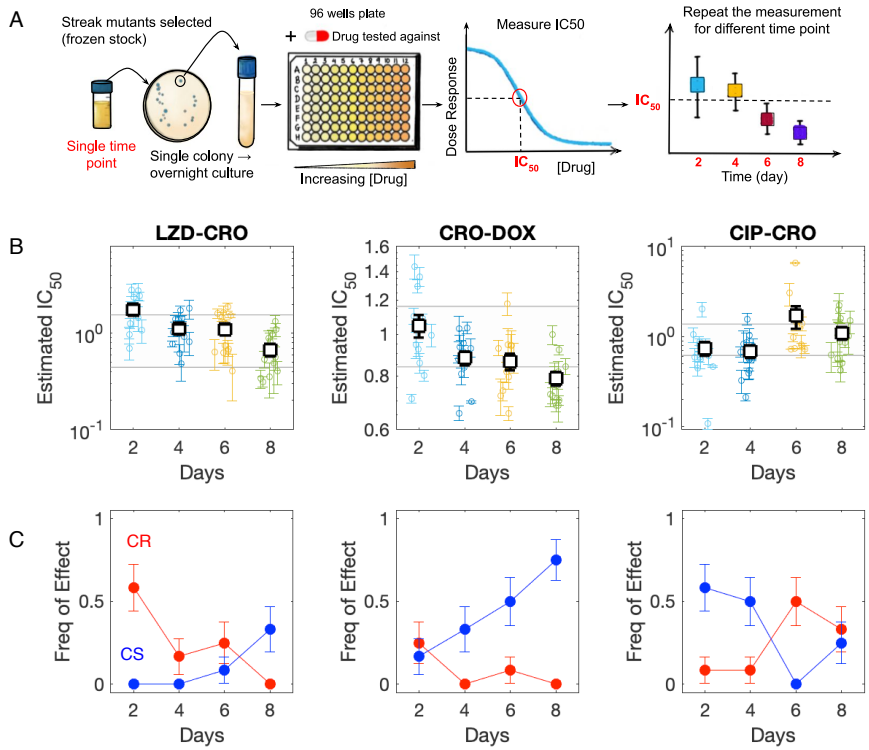

Fig 3. Collateral effects are dynamic within individual populations. (A): Samples from a single evolved population at days 2, 4, 6, and 8 are plated and 12 colonies from each time point are selected for phenotyping (IC_{50} characterization). **(B):** Measured IC_{50} values for 12 isolates at each of 4 different time points from populations adapted to LZD (left), CRO (middle), and CIP (right) and exposed to CRO (left), DOX (middle), and CRO (right). Shaded region indicates IC_{50} of ancestor strain ($\pm$ 3 standard error). Individual points represent the mean IC_{50} ($\pm$ standard error from 4 technical replicates) for a single colony. Open squares represent the population mean–that is, the mean across all colonies (error bars are $\pm$ standard deviation of the population). **(C):** Frequency of colonies exhibiting collateral sensitivity (blue) or collateral resistance (red) over time. See also Figure S5.

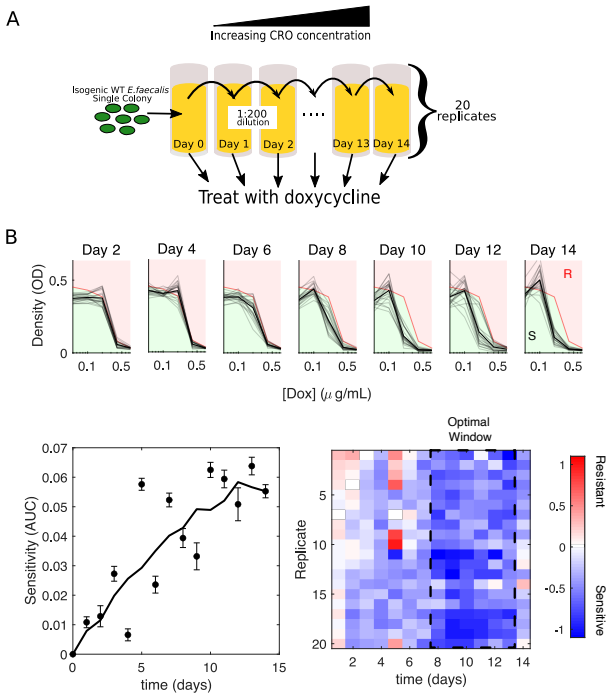

Fig 4. Success of switching to a second antibiotic is contingent on temporally dynamic collateral effects. (A) Twenty replicate populations of *E. faecalis* V583 were exposed to increasing concentrations of the antibiotic ceftrixone (CRO) over the course of 14 days via serial passage. At the end of each day a sample of the population was isolated and cultured in a range of doxycycline (DOX) concentrations for 24 hours. **(B) Top:** Density (OD) after 24 hours vs drug (DOX) concentration for all 20 populations (light gray), and the mean over the 20 populations (dark black) at different days of the evolution experiment. For comparison, the dose response curve in the ancestral strain (red curve) divides the space into regions of increased resistance (red) and increased sensitivity (green). **(B) Bottom left:** Average sensitivity over 20 populations (error bar standard error of the mean) at different time points. Sensitivity is defined as the difference in area under the curve between the ancestral dose response curve and the dose response curve of the population in question between the lowest ([Dox]=0.05 µg/mL) and highest ([Dox]=0.8 µg/mL) nonzero drug concentrations. Solid line is a moving average. **(B) Bottom right:** Collateral effects (quantified, as before, by $\log_2$-transformed fold change in the IC_{50}). Dashed region highlights a transient six-day window where collateral sensitivity is more pronounced.

the timing that can potentially optimize resistance to the applied drugs.

Success of switching to a second antibiotic is contingent on temporally dynamic collateral effects.

To investigate the effects of drug timing experimentally, we designed an evolution experiment (Fig 4A) meant to approximate a hypothetical drug-switching protocol involving two drugs (CRO and DOX) suggested by simulations to be particularly sensitive to the timing of drug switching (i.e. large difference between best and worst treatments, Fig S6C). Similar to our previous experiments, we performed serial passage evolution using escalating concentrations of the antibiotic CRO but now for a total period of 14 days. At the end of each day, we exposed a diluted sample of that population to varying concentrations of a second antibiotic, DOX, to probe how switching to a second drug may have increased or decreased the treatment efficacy. The entire process was repeated for 20 independent populations to quantify evolutionary variability (Fig 4B).

To quantify sensitivity to DOX, we calculated both a global area-under-the-curve sensitivity score, where we take the difference between the area under the dose response curve of the ancestral strain and each evolved population (Fig 4B, bottom left), as well as the previously described collateral effect metric (i.e. the log-scaled fold change in half-maximal inhibitory concentration). Both metrics show that populations adapted to CRO become increasingly sensitized to DOX over time. The sensitivity is particularly notable between days 8 and 13, where the mean collateral sensitivity (across replicate populations) is maximized before starting to decline (Fig 4B, bottom right; post-hoc pairwise comparisons following 1-way Anova identify days 8-13 as a statistically distinct cluster; see SI Supplemental Tables). Switching to DOX at time points before or after that window produces different levels of average sensitivty and even leads to resistance in some populations. These results indicate that the effects of a new antibiotic can vary considerably depending on when, along the adaptation trajectory, the new drug is applied.

Discussion

Our work provides systematic evidence of temporal collateral drug effects in the pathogen *E. faecalis*. The time-dependent nature of collateral sensitivity and collateral resistance presents both additional challenges and new opportunities for designing multi-drug therapies to slow resistance. Full optimization of sequential drug therapies will likely involve not merely static, end-point measurements of collateral effects, but a full description of their temporal development.

The goal of this study was to broadly survey phenotypic resistance patterns over time in a systematic way. This approach comes with obvious drawbacks, and we are left with many unanswered questions. Most notably, our work does not provide any information about the molecular mechanisms underlying the collateral effects; such insight, while hard won even for a single pair of drugs, will be essential to fully exploit the phenotypic effects observed here. In addition, we focused on a single bacterial species, and all experiments were performed starting from the ancestral V583 *E. faecalis* strain. It is not clear how the results might change in a different strain or species, though data from several recent studies suggest the presence of dynamic features in collateral profiles in other species [10,35,51,53]. Indeed, recent work underscores just how important genotype can be in antibiotic evolvability [71], and the search for more general patterns is ongoing [35,51,53]. It is also possible that at least some of the trends we observe are specific to the precise laboratory evolution protocol used here, where drug is systematically increased over time following serial dilution.Future work may aim to identify how these patterns change in cells from different physiological states (e.g. biofilm [72]) or under different modes of selection pressure [73].

Finally, it is important to keep in mind the scope of our work. These evolution experiments are done in a highly controlled laboratory environment. Our protocols are not meant to guide clinicians, but instead focus on whether or not collateral profiles changed even in the simplest of drug-evolution environments – free, for example, of the important but difficult-to-quantify interactions between host and pathogen. Translating these results into a clinically accurate model would require additional work to understand the mechanistic, clinical, and even theoretical principles governing drug sequence optimization. This work serves as a reminder of the complexities of evolution and the still long path we must walk to confidently prescribe effective dosing schedules in patients. At the same time, the results highlight the rich dynamical behavior of collateral sensitivity in even simplified laboratory populations, offering a largely unexplored frontier for evolution-based control strategies.

Materials and methods

Strains, antibiotics, and media

All resistance evolution lineages were derived from an *E faecalis* V583 ancestor, a fully sequenced clinical isolate with vancomycin resistance [74]. The 5 antibiotics used in this study and their mechanisms of action are listed in Table 1. Antibiotics were prepared from powder stock and stored at appropriate temperature. Evolution and IC_{50} measurements were conducted in BHI (brain heart infusion).

Laboratory evolution experiments

Evolution experiments were performed in replicates of four. Daily serial passage evolutions were conducted in 1 mL BHI medium in 96-well plates with a maximum volume of 2 mL. Each day populations were grown in three antibiotic concentrations spanning sub- and super-MIC doses. After approximately 16 hours of incubation at 37°C, the well with the highest drug concentration that contained visible growth was propagated into three new concentrations (typically one-half, 2x and 4x the highest concentration that had visible growth). A 1/200 dilution was used as an inoculum for the next day's evolution plate. This process was repeated for 8 days for the multi-drug study and 14 days for the CRO/DOX study. All strains were stocked in 30% glycerol and subsequently plated on pure BHI plates for further experimentation. A single colony was selected for IC_{50} determination. To help ensure no contamination occured, cells were regularly plated and visualized using DIC microscopy to ensure *E. faecalis* morphology.

Measuring drug resistance and sensitivity

IC_{50} determination experiments were performed in 96-well plates by exposing each strain to a drug gradient consisting of between 6-14 concentrations, typically in linear dilution series prepared in BHI medium with a total volume of 205 µL (200 µL BHI, 5 µL of 1.5 OD cells) in each well. After 20 hours, we measured the OD at 600 nm via an Enspire Multi-modal Plate Reader (Perkin Elmer) with an automated plate stacker. OD measurements for each drug were normalized by the OD600 in the absence of drug.

In order to quantify resistance to each drug, the OD600-generated dose-response curve was fit to a Hill-like function $f(x) = (1 + (\frac{x}{K})^h)^{-1}$ using a nonlinear least squares fitting. K is the IC_{50} and h is a Hill coefficient that represents the steepness of the dose-response curve. Strains were deemed "collaterally resistant" or "collaterally sensitive" if its IC_{50} had increased or decreased by more than 3 times the standard error of the wild-type mean IC_{50}. In previous work, we chose this threshold because it minimized the number of false positives (e.g. all measurements of IC_{50} in the ancestor strains, across all drugs, fell within this $\pm 3\sigma_{WT}$ window) [40, 44]. All dose response curves were measured in technical replicates of 3 or 4.

Logistic regressions for estimating frequency trends

To characterize trends in the frequency of resistance (CR) or sensitivity (CS) we used standard logistic regression. Specifically, we assume the classic logit model where $\ln p/(1-p) = c_1 + c_2 X$, with p the probability of CR (or CS), c_1 and c_2 regression coefficients, and X the predictor variable of interest (either resistance to the selecting drug, as in Figure 2, or time, as in Figure 3. An increasing trend corresponds to $c_2 > 0$ and a decreasing trend to $c_2 < 0$. P-values (p_{value}) are given for each regression in the corresponding figure caption and in SI Supplemental Tables.

Acknowledgments

This work was supported by NIH R35 GM124875 (to KBW).

References

1. Boucher HW, Talbot GH, Bradley JS, Edwards JE, Gilbert D, Rice LB, et al. Bad bugs, no drugs: no ESKAPE! An update from the Infectious Diseases Society of America. Clinical infectious diseases. 2009;48(1):1–12.

2. Goldberg DE, Siliciano RF, Jacobs Jr WR. Outwitting evolution: fighting drug-resistant TB, malaria, and HIV. Cell. 2012;148(6):1271–1283.

3. Pfaller MA. Antifungal drug resistance: mechanisms, epidemiology, and consequences for treatment. The American journal of medicine. 2012;125(1):S3–S13.

4. Raviglione M, Marais B, Floyd K, Lönnroth K, Getahun H, Migliori GB, et al. Scaling up interventions to achieve global tuberculosis control: progress and new developments. The Lancet. 2012;379(9829):1902–1913.

5. Borst P. Cancer drug pan-resistance: pumps, cancer stem cells, quiescence, epithelial to mesenchymal transition, blocked cell death pathways, persisters or what? Open biology. 2012;2(5):120066.

6. Pluchino KM, Hall MD, Goldsborough AS, Callaghan R, Gottesman MM. Collateral sensitivity as a strategy against cancer multidrug resistance. Drug Resistance Updates. 2012;15(1-2):98–105.

7. Brown EM, Nathwani D. Antibiotic cycling or rotation: a systematic review of the evidence of efficacy. Journal of Antimicrobial Chemotherapy. 2005;55(1):6–9. doi:10.1093/jac/dkh482.

8. Bergstrom CT, Lo M, Lipsitch M. Ecological theory suggests that antimicrobial cycling will not reduce antimicrobial resistance in hospitals. Proceedings of the National Academy of Sciences. 2004;101(36):13285–13290. doi:10.1073/pnas.0402298101.

9. Nichol D, Jeavons P, Fletcher AG, Bonomo RA, Maini PK, Paul JL, et al. Steering evolution with sequential therapy to prevent the emergence of bacterial antibiotic resistance. PLoS Comput Biol. 2015;11(9):e1004493.

10. Batra A, Roemhild R, Rousseau E, Franzenburg S, Niemann S, Schulenburg H. High potency of sequential therapy with only β-lactam antibiotics. Elife. 2021;10:e68876.

11. Zhang Q, Lambert G, Liao D, Kim H, Robin K, Tung Ck, et al. Acceleration of emergence of bacterial antibiotic resistance in connected microenvironments. Science. 2011;333(6050):1764–1767.

12. Baym M, Lieberman TD, Kelsic ED, Chait R, Gross R, Yelin I, et al. Spatiotemporal microbial evolution on antibiotic landscapes. Science. 2016;353(6304):1147–1151.

13. De Jong MG, Wood KB. Tuning spatial profiles of selection pressure to modulate the evolution of drug resistance. Physical review letters. 2018;120(23):238102.

14. Feder AF, Harper KN, Brumme CJ, Pennings PS. Understanding patterns of HIV multi-drug resistance through models of temporal and spatial drug heterogeneity. eLife. 2021;10:e69032. doi:10.7554/eLife.69032.

15. Yurtsev EA, Chao HX, Datta MS, Artemova T, Gore J. Bacterial cheating drives the population dynamics of cooperative antibiotic resistance plasmids. Molecular systems biology. 2013;9(1):683.

16. Meredith HR, Lopatkin AJ, Anderson DJ, You L. Bacterial temporal dynamics enable optimal design of antibiotic treatment. PLoS Comput Biol. 2015;11(4):e1004201.

17. Meredith HR, Srimani JK, Lee AJ, Lopatkin AJ, You L. Collective antibiotic tolerance: mechanisms, dynamics and intervention. Nature chemical biology. 2015;11(3):182.

18. Farrokhian N, Maltas J, Dinh M, Durmaz A, Ellsworth P, Hitomi M, et al. Measuring competitive exclusion in non–small cell lung cancer. Science Advances. 2022;8(26):eabm7212.

19. Gatenby RA, Silva AS, Gillies RJ, Frieden BR. Adaptive therapy. Cancer research. 2009;69(11):4894–4903.

20. West J, You L, Zhang J, Gatenby RA, Brown JS, Newton PK, et al. Towards multidrug adaptive therapy. Cancer research. 2020;80(7):1578–1589.

21. Hansen E, Karslake J, Woods RJ, Read AF, Wood KB. Antibiotics can be used to contain drug-resistant bacteria by maintaining sufficiently large sensitive populations. PLoS biology. 2020;18(5):e3000713.

22. Zimmer A, Katzir I, Dekel E, Mayo AE, Alon U. Prediction of multidimensional drug dose responses based on measurements of drug pairs. Proceedings of the National Academy of Sciences. 2016;113(37):10442–10447.

23. Wood K, Nishida S, Sontag ED, Cluzel P. Mechanism-independent method for predicting response to multidrug combinations in bacteria. Proceedings of the National Academy of Sciences. 2012;109(30):12254–12259.

24. Torella JP, Chait R, Kishony R. Optimal drug synergy in antimicrobial treatments. PLoS Comput Biol. 2010;6(6):e1000796.

25. Michel JB, Yeh PJ, Chait R, Moellering RC, Kishony R. Drug interactions modulate the potential for evolution of resistance. Proceedings of the National Academy of Sciences. 2008;105(39):14918–14923.

26. Dean Z, Maltas J, Wood K. Antibiotic interactions shape short-term evolution of resistance in E. faecalis. PLoS pathogens. 2020;16(3):e1008278.

27. Jahn LJ, Simon D, Jensen M, Bradshaw C, Ellabaan MMH, Sommer MOA. Compatibility of evolutionary responses to constituent antibiotics drive resistance evolution to drug pairs. Molecular Biology and Evolution. 2021;.

28. Tekin E, Beppler C, White C, Mao Z, Savage VM, Yeh PJ. Enhanced identification of synergistic and antagonistic emergent interactions among three or more drugs. Journal of The Royal Society Interface. 2016;13(119):20160332.

29. Gjini E, Wood KB. Price equation captures the role of drug interactions and collateral effects in the evolution of multidrug resistance. Elife. 2021;10:e64851.

30. Barbosa C, Römhild R, Rosenstiel P, Schulenburg H. Evolutionary stability of collateral sensitivity to antibiotics in the model pathogen Pseudomonas aeruginosa. Elife. 2019;8:e51481.

31. Maltas J, McNally DM, Wood KB. Evolution in alternating environments with tunable interlandscape correlations. Evolution. 2021;75(1):10–24.

32. Lázár V, Pal Singh G, Spohn R, Nagy I, Horváth B, Hrtyan M, et al. Bacterial evolution of antibiotic hypersensitivity. Molecular systems biology. 2013;9(1):700.

33. Lázár V, Nagy I, Spohn R, Csörgő B, Györkei Á, Nyerges Á, et al. Genome-wide analysis captures the determinants of the antibiotic cross-resistance interaction network. Nature communications. 2014;5(1):1–12.

34. Imamovic L, Sommer MO. Use of collateral sensitivity networks to design drug cycling protocols that avoid resistance development. Science translational medicine. 2013;5(204):204ra132–204ra132.

35. Imamovic L, Ellabaan MMH, Machado AMD, Citterio L, Wulff T, Molin S, et al. Drug-driven phenotypic convergence supports rational treatment strategies of chronic infections. Cell. 2018;172(1-2):121–134.

36. Roemhild R, Linkevicius M, Andersson DI. Molecular mechanisms of collateral sensitivity to the antibiotic nitrofurantoin. PLoS biology. 2020;18(1):e3000612.

37. Zhao B, Sedlak JC, Srinivas R, Creixell P, Pritchard JR, Tidor B, et al. Exploiting temporal collateral sensitivity in tumor clonal evolution. Cell. 2016;165(1):234–246.

38. Ardell SM, Kryazhimskiy S. The population genetics of collateral resistance and sensitivity. eLife. 2021;10:e73250.

39. Herencias C, Rodríguez-Beltrán J, León-Sampedro R, Alonso-del Valle A, Palkovičová J, Cantón R, et al. Collateral sensitivity associated with antibiotic resistance plasmids. Elife. 2021;10:e65130.

40. Maltas J, Wood KB. Pervasive and diverse collateral sensitivity profiles inform optimal strategies to limit antibiotic resistance. PLoS biology. 2019;17(10):e3000515.

41. Barbosa C, Trebosc V, Kemmer C, Rosenstiel P, Beardmore R, Schulenburg H, et al. Alternative evolutionary paths to bacterial antibiotic resistance cause distinct collateral effects. Molecular biology and evolution. 2017;34(9):2229–2244.

42. Oz T, Guvenek A, Yildiz S, Karaboga E, Tamer YT, Mumcuyan N, et al. Strength of selection pressure is an important parameter contributing to the complexity of antibiotic resistance evolution. Molecular biology and evolution. 2014;31(9):2387–2401.

43. Nichol D, Rutter J, Bryant C, Hujer AM, Lek S, Adams MD, et al. Antibiotic collateral sensitivity is contingent on the repeatability of evolution. Nature communications. 2019;10(1):1–10.

44. Maltas J, Krasnick B, Wood KB. Using selection by nonantibiotic stressors to sensitize bacteria to antibiotics. Molecular biology and evolution. 2020;37(5):1394–1406.

45. Bhardwaj P, Hans A, Ruikar K, Guan Z, Palmer KL. Reduced chlorhexidine and daptomycin susceptibility in vancomycin-resistant Enterococcus faecium after serial chlorhexidine exposure. Antimicrobial agents and chemotherapy. 2018;62(1).

46. Lázár V, Martins A, Spohn R, Daruka L, Grézal G, Fekete G, et al. Antibiotic-resistant bacteria show widespread collateral sensitivity to antimicrobial peptides. Nature microbiology. 2018;3(6):718–731.

47. Knöppel A, Näsvall J, Andersson DI. Evolution of antibiotic resistance without antibiotic exposure. Antimicrobial agents and chemotherapy. 2017;61(11).

48. Creamer KE, Ditmars FS, Basting PJ, Kunka KS, Hamdallah IN, Bush SP, et al. Benzoate-and salicylate-tolerant strains of Escherichia coli K-12 lose antibiotic resistance during laboratory evolution. Applied and environmental microbiology. 2017;83(2):e02736–16.

49. Moore JP, Li H, Engmann ML, Bischof KM, Kunka KS, Harris ME, et al. Inverted regulation of multidrug efflux pumps, acid resistance, and porins in benzoate-evolved Escherichia coli K-12. Applied and environmental microbiology. 2019;85(16):e00966–19.

50. Iram S, Dolson E, Chiel J, Pelesko J, Krishnan N, Güngör Ö, et al. Controlling the speed and trajectory of evolution with counterdiabatic driving. Nature Physics. 2020; p. 1–8.

51. Roemhild R, Andersson DI. Mechanisms and therapeutic potential of collateral sensitivity to antibiotics. PLoS Pathogens. 2021;17(1):e1009172.

52. de Evgrafov MCR, Faza M, Asimakopoulos K, Sommer MO. Systematic investigation of resistance evolution to common antibiotics reveals conserved collateral responses across common human pathogens. Antimicrobial Agents and Chemotherapy. 2020;65(1).

53. Beckley AM, Wright ES. Identification of antibiotic pairs that evade concurrent resistance via a retrospective analysis of antimicrobial susceptibility test results. The Lancet Microbe. 2021;2(10):e545–e554.

54. Zwep LB, Haakman Y, Duisters KL, Meulman JJ, Liakopoulos A, van Hasselt JC. Identification of antibiotic collateral sensitivity and resistance interactions in population surveillance data. JAC-antimicrobial resistance. 2021;3(4):dlab175.

55. Dhawan A, Nichol D, Kinose F, Abazeed ME, Marusyk A, Haura EB, et al. Collateral sensitivity networks reveal evolutionary instability and novel treatment strategies in ALK mutated non-small cell lung cancer. Scientific reports. 2017;7(1):1–9.

56. Gilmore MS, Clewell DB, Ike Y, Shankar N. Enterococci: From Commensals to Leading Causes of Drug Resistant Infection [Internet]. 2014;.

57. O'Driscoll T, Crank CW. Vancomycin-resistant enterococcal infections: epidemiology, clinical manifestations, and optimal management. Infection and drug resistance. 2015;8:217.

58. Cetinkaya Y, Falk P, Mayhall CG. Vancomycin-resistant enterococci. Clinical microbiology reviews. 2000;13(4):686–707.

59. Huycke MM, Sahm DF, Gilmore MS. Multiple-drug resistant enterococci: the nature of the problem and an agenda for the future. Emerging infectious diseases. 1998;4(2):239.

60. Palmer KL, Daniel A, Hardy C, Silverman J, Gilmore MS. Genetic basis for daptomycin resistance in enterococci. Antimicrobial agents and chemotherapy. 2011;55(7):3345–3356.

61. Miller C, Kong J, Tran TT, Arias CA, Saxer G, Shamoo Y. Adaptation of Enterococcus faecalis to daptomycin reveals an ordered progression to resistance. Antimicrobial agents and chemotherapy. 2013;57(11):5373–5383.

62. Munoz-Price LS, Lolans K, Quinn JP. Emergence of resistance to daptomycin during treatment of vancomycin-resistant Enterococcus faecalis infection. Clinical infectious diseases. 2005;41(4):565–566.

63. Balli EP, Venetis CA, Miyakis S. Systematic review and meta-analysis of linezolid versus daptomycin for treatment of vancomycin-resistant enterococcal bacteremia. Antimicrobial agents and chemotherapy. 2014;58(2):734–739.

64. Auckland C, Teare L, Cooke F, Kaufmann ME, Warner M, Jones G, et al. Linezolid-resistant enterococci: report of the first isolates in the United Kingdom. Journal of Antimicrobial Chemotherapy. 2002;50(5):743–746.

65. Kelesidis T, Humphries R, Uslan DZ, Pegues DA. Daptomycin nonsusceptible enterococci: an emerging challenge for clinicians. Clinical Infectious Diseases. 2011;52(2):228–234.

66. Du D, Wang-Kan X, Neuberger A, van Veen HW, Pos KM, Piddock LJ, et al. Multidrug efflux pumps: structure, function and regulation. Nature Reviews Microbiology. 2018;16(9):523–539.

67. Jonas BM, Murray BE, Weinstock GM. Characterization of emeA, anorA Homolog and Multidrug Resistance Efflux Pump, in Enterococcus faecalis. Antimicrobial Agents and Chemotherapy. 2001;45(12):3574–3579.

68. Lee EW, Huda MN, Kuroda T, Mizushima T, Tsuchiya T. EfrAB, an ABC multidrug efflux pump in Enterococcus faecalis. Antimicrobial agents and chemotherapy. 2003;47(12):3733–3738.

69. Duval V, Lister IM. MarA, SoxS and Rob of Escherichia coli–Global regulators of multidrug resistance, virulence and stress response. International journal of biotechnology for wellness industries. 2013;2(3):101.

70. Sukhai M, Piquette-Miller M. Regulation of the multidrug resistance genes by stress signals. J Pharm Pharm Sci. 2000;3(2):268–280.

71. Card KJ, LaBar T, Gomez JB, Lenski RE. Historical contingency in the evolution of antibiotic resistance after decades of relaxed selection. PLoS biology. 2019;17(10):e3000397.

72. Santos-Lopez A, Marshall CW, Scribner MR, Snyder DJ, Cooper VS. Evolutionary pathways to antibiotic resistance are dependent upon environmental structure and bacterial lifestyle. Elife. 2019;8.

73. Toprak E, Veres A, Michel JB, Chait R, Hartl DL, Kishony R. Evolutionary paths to antibiotic resistance under dynamically sustained drug selection. Nature genetics. 2012;44(1):101–105.

74. Sahm DF, Kissinger J, Gilmore MS, Murray PR, Mulder R, Solliday J, et al. In vitro susceptibility studies of vancomycin-resistant Enterococcus faecalis. Antimicrobial agents and chemotherapy. 1989;33(9):1588–1591.

75. Cordell HJ. Epistasis: what it means, what it doesn't mean, and statistical methods to detect it in humans. Human molecular genetics. 2002;11(20):2463–2468.

76. Russ D, Kishony R. Additivity of inhibitory effects in multidrug combinations. Nature microbiology. 2018;3(12):1339–1345.

77. Roemhild R, Gokhale CS, Dirksen P, Blake C, Rosenstiel P, Traulsen A, et al. Cellular hysteresis as a principle to maximize the efficacy of antibiotic therapy. Proceedings of the National Academy of Sciences. 2018;115(39):9767–9772.